https://doi.org/10.22226/2410-3535-2021-4-467-472 PACS: 61.72.Lk, 62.20.F

The role of a shear planar mesodefect in the nucleation of a crack at a grain junction due to athermal grain boundary sliding

V. N. Perevezentsev, S. V. Kirikov, J. V. Svirina†

†j.svirina@mail.ru

Mechanical Engineering Research Institute of the RAS — Branch of Federal Research Center "Institute of Applied Physics of the RAS", Nizhny Novgorod, 603024, Russia

Ductile fracture of polycrystalline metals is usually preceded by a long deformation stage, during which grains of polycrystal are gradually divided into mutually misoriented regions (fragments) separated by strain-induced grain boundaries. The size of these regions usually does not exceed 0.2 – 0.4 mm. At such small sizes of fragments, classical models of crack nucleation based on the concept of lattice dislocation pile-ups retarded by grain boundaries become incorrect. In recent years, models have been developed to describe the nucleation of cracks under the action of elastic stress fields of rotational and shear-type mesodefects formed at the grain junctions and grain boundaries due to inhomogeneous plastic deformation in the ensemble of polycrystal grains. In this paper we consider the possibility of the nucleation of microcracks at the grain junction due to athermal sliding along the grain boundary, containing a planar mesodefect of the shear-type induced by strain. It is assumed that a planar mesodefect, represented in the initial state by uniformly distributed glissile components of orientational misfit dislocations, loses its stability when the external stress exceeds a certain threshold value. As a result of the strain-induced grain boundary sliding and plastic shear retarding, a stress concentrator arises near the triple junction of grains, creating conditions for the appearance of a Zener crack. The dependences of the critical external stress for the nucleation of microcracks on the length of the mesodefect, its strength and the threshold stress of athermal sliding are obtained. It is shown that the presence of a mesodefect at the grain boundary can lead to a significant decrease of the crack nucleation stress in comparison with the case of pure grain boundary sliding. It is concluded that the proposed model can be considered as one of the possible mechanisms for the nucleation of microcracks in materials with a fragmented structure.

Keywords: grain boundaries, dislocations, strain induced mesodefects, grain boundary sliding, fracture.

УДК: 548.4, 539.372

Роль сдвигового планарного мезодефекта в зарождении трещины на стыке зерен из-за атермического зернограничного скольжения

Перевезенцев В. Н., Кириков С. В., Свирина Ю. В.†

Институт машиностроения РАН — филиал Федерального исследовательского центра «Институт прикладной физики РАН», Нижний Новгород, 603024, Россия

Пластическому разрушению поликристаллических металлов обычно предшествует длительная стадия деформации, во время которой зерна поликристалла постепенно разделяются на взаимно разориентированные области (фрагменты), разделенные деформационными границами зерен. Размер этих областей обычно не превышает 0.2 – 0.4 мкм. При столь малых размерах фрагментов классические модели зарождения трещин, основанные на концепции скоплений решеточных дислокаций, задерживаемых границами зерен, становятся некорректными. В последние годы разработаны модели для описания зарождения трещин под действием полей упругих напряжений поворотных и сдвиговых мезодефектов, образующихся на стыках зерен и в границах зерен в результате неоднородной пластической деформации в ансамбле зерен поликристалла. В данной работе рассматривается возможность зарождения микротрещин на стыке зерен из-за атермического скольжения по границе зерен, содержащей пла-

нарный мезодефект сдвигового типа, индуцированный деформацией. Предполагается, что плоский мезодефект, представленный в исходном состоянии равномерно распределенными скользящими компонентами дислокаций ориентационного несоответствия, теряет устойчивость, когда внешнее напряжение превышает определенное пороговое значение. В результате вызванного деформацией зернограничного скольжения и замедления пластического сдвига вблизи тройного стыка зерен возникает концентратор напряжений, создавая условия для возникновения трещины Зенера. Получены зависимости критического внешнего напряжения для зарождения микротрещин от длины мезодефекта, его прочности и порогового напряжения атермического скольжения. Показано, что наличие мезодефекта на границе зерен может привести к значительному снижению напряжения зарождения трещины по сравнению со случаем чистого зернограничного скольжения. Сделан вывод о том, что предложенная модель может рассматриваться как один из возможных механизмов зарождения микротрещин в материалах с фрагментированной структурой.

Ключевые слова: границы зерен, дислокации, деформационные мезодефекты, зернограничное скольжение, разрушение.

1. Introduction

As the results of experimental and theoretical investigations show, ductile fracture of polycrystalline metals is usually preceded by a rather long deformation stage, during which grains of polycrystal are gradually divided into mutually misoriented regions (fragments) separated by strain-induced grain boundaries [1–2]. The size of these regions usually does not exceed 0.2–0.4 μm. At such small sizes of fragments, classical models of crack nucleation based on the concept of lattice dislocation pile-ups retarded by grain boundaries become incorrect. In this regard, in recent years, models have been developed to describe the nucleation of cracks under the action of the elastic stress fields of mesodefects. These mesodefects are formed at grain boundaries and at grain junctions due to inhomogeneous plastic deformation in the ensemble of polycrystal grains. Thus, the difference of plastic distortion in neighboring grains creates additional misorientations at the grain boundaries. The mismatch of misorientations at the grain junctions leads to the appearance of strain induced junction disclinations there [3–5]. In addition to these linear rotational-type mesodefects, planar shear-type mesodefects appear at the boundaries during deformation in the form of plastic shears uniformly distributed along the boundaries. The elastic stress fields from these mesodefects increase with deformation.

Stress relaxation can take place due to accommodative plastic deformation, which leads to the appearance of specific dislocation structures near mesodefects (broken dislocation walls, accommodative slip bands, etc.) [1,5,6]. However, if the processes of plastic accommodation are exhausted, the only way for the relaxation of the elastic stresses of mesodefects is the nucleation of microcracks. The currently available theoretical investigations of the role of rotational shear mesodefects in the nucleation of microcracks are limited to consideration of simple configurations. Thus, the conditions for the appearance of microcracks in the elastic field of a single wedge disclination and a biaxial dipole of disclinations were considered in [7–9]. The conditions for the nucleation of a Zener-Griffith crack near a disclination dipole were analyzed in [10]. The analysis of the conditions for the existence of equilibrium stable cracks in the field of stresses from a mesodefect, which is represented by a superposition of a dipole of wedge disclinations and a planar shear mesodefect is carried out in [11]. Models of crack nucleation as a result of athermal grain boundary sliding (GBS) were considered in [12,13].

An analysis of the conditions for crack nucleation near triple junctions of grains in polycrystalline silicon due to pure GBS was carried out in [12]. A model of crack nucleation in the elastic field of a disclination dipole formed at the grain junction during GBS was considered in [13]. Experimental evidence of the possibility of GBS at relatively low temperatures, at which the influence of diffusion processes can be neglected, was obtained in [14–19]. Thus, GBS was observed at a temperature of $\approx 0.15T_m$ in nanostructured pure titanium VT1-0 containing a high fraction of nonequilibrium strain induced grain boundaries using the methods based on the detection of mutual displacement of preliminarily applied scratch marks [14]. The sliding of grain boundaries was observed at room temperature in zinc [15], magnesium [16], alloys based on them [16–18] and titanium [19]. Electron microscopic studies of GBS in the Ti-6Al-4V alloy deformed by uniaxial tension at room temperature [20] revealed its close relationship with intragranular slip. It was found that sliding is initiated in parts of the boundary accumulating lattice dislocations incoming in the boundary from the body of grains. As a rule, sliding is observed in the places where slip bands come into the boundary. Note that this type of GBS is most likely in highly deformed metals and alloys with a large fraction of nonequilibrium strain induced grain boundaries, characterized by a high density of orientational misfit dislocations. In this paper, we consider the role of a strain-induced planar shear mesodefect in the nucleation of microcracks at the junction of grain boundaries due to athermal GBS.

2. Description of the model

The analysis of strain induced rotational shear mesodefects in the general case was carried out in [3]. Within the framework of the 2D model, it is sufficient to consider the boundary with triple grain junctions on both sides (Fig. 1a), containing uniformly distributed sessile and glissile components of orientational misfit dislocations induced into the boundary during homogeneous plastic deformation of grains adjacent to the boundary.

Sessile dislocations with the density of the Burgers vector $\mathbf{w}_N$ form the rotational type mesodefect and its elastic stress fields are equivalent to the fields of the dipole of

wedge disclinations. The Frank vector of each disclination is determined by the formulas:

$$\mathbf{w}_d(\mathbf{r}_1)=\frac{\mathbf{w}_N\times(\mathbf{r}_1-\mathbf{r}_2)}{|\mathbf{r}_1-\mathbf{r}_2|};\ \mathbf{w}_d(\mathbf{r}_2)=\frac{\mathbf{w}_N\times(\mathbf{r}_2-\mathbf{r}_1)}{|\mathbf{r}_2-\mathbf{r}_1|},$$

where $\mathbf{w}_d(\mathbf{r}_1)$ and $\mathbf{w}_d(\mathbf{r}_2)$ are the Frank vectors of disclinations located at points with radius vectors $\mathbf{r}_1$ and $\mathbf{r}_2$ correspondingly. The glissile components of dislocations with the density of the Burgers vector $\mathbf{w}_\tau$ represent a planar shear mesodefect. The vectors $\mathbf{w}_d$ and $\mathbf{w}_\tau$ are the strengths of the corresponding mesodefects. Let us consider the conditions of the microcrack nucleation in the triple junction during athermal GBS. Depending on the initial parameters of the model, GBS may be carried out by pure GBS (at $\mathbf{w}_\tau=0$), by the motion of dislocations of the mesodefect (strain induced GBS), or both strain-induced GBS and pure GBS. Pure GBS is provided by the nucleation of pares of unlike virtual glissile dislocations in the grain boundary. A schematic representation of the dislocations providing strain induced GBS and pure GBS is shown in Fig. 2. We assume that the mutual displacement of grains at any point of the considered boundary is possible only if the shear stress at this point exceeds a certain threshold stress τ_0. The value τ_0 is close to the theoretical shear strength for the equilibrium grain boundary. However, the threshold stress of GBS can be significantly lower for nonequilibrium strain-induced high angle grain boundaries, containing a large number of deformation defects, or in the presence of segregations of impurity atoms, which cause weakening of interatomic bonds across the boundary.

Therefore, in further consideration, we will consider it as a variable parameter. The shear stress τ^Σ at an arbitrary point of the boundary is a sum of the external stress τ^{ext} and the internal stress τ^{int} from dislocations of the mesodefect providing strain-induced GBS and from virtual dislocations providing pure GBS when it takes place. As a result of sliding and retardation of plastic shear near the triple junctions, a distribution of the density of the Burgers vector of virtual glissile dislocations comes to an equilibrium, at which the total shear stress at each point of the grain boundary is less or equal to τ_0. Note that a disclination dipole does not create shear stresses at the boundary within the considered configuration of the mesodefect (Fig. 1b). According to the idea of Zener [21], we will consider the criterion for the nucleation of microcracks as a condition necessary for the appearance of a superdislocation with the Burgers vector $B\geq 2b$ in the head of the pile-up of virtual glissile dislocations located in the region of length $2r_0$ (b is the Burgers vector and r_0 is the radius of the lattice dislocation core).

3. Calculation of the distribution function of glissile dislocations

In the initial state, virtual dislocations of the planar shear mesodefect are uniformly distributed with the density of the Burgers vector w_τ along the boundary, where w_τ is the value of $\mathbf{w}_\tau$ projection on the axis Ox (Fig. 1b). The mesodefect becomes unstable if the total shear stress τ^Σ, acting on any dislocation, exceeds the threshold stress τ_0. The new equilibrium distribution of the density of virtual dislocations of the Burgers vector $\rho(x)$, arising due to the dislocations motion and retarding of GBS by triple junctions, must satisfy the following conditions:

a) the total Burgers vector of virtual dislocations should be equal to the total Burgers vector of dislocations of the initial shear mesodefect:

$$\int_{-a}^{a}\rho(x)dx=2aw_\tau,$$

b) for each point of the boundary (points $x=\pm a$ excepted), τ^Σ should not exceed the threshold stress τ_0:

$$\left|\frac{G}{2\pi(1-\nu)}\int_{-a}^{a}\frac{\rho(x')dx'}{x'-x}+\tau^{ext}\right|\leq\tau_0,\quad\forall x\in(-a\quad a).$$

The initial shear mesodefect is approximated by n_w equidistantly distributed virtual glissile dislocations with the Burgers vector b_d, where $n_w=2aw_\tau/b_d$. The density of the Burgers vector of dislocations $\rho_n(x_i)$ we define as:

$$\rho_n(x_i)=\frac{(b_d)_i}{x_{i+1}-x_i},\ i=\overline{1,n-1},$$

where x_i are the coordinate of i^{th} dislocation known from the numerical calculation with the Burgers vector $(b_d)_i=\pm b_d$, n is the total number of virtual dislocations of the mesodefect

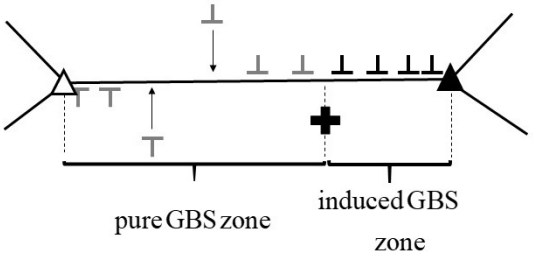

Fig. 2. Schematic representation of dislocations providing strain induced GBS (dislocations colored in black) and pure GBS (dislocations colored in gray).

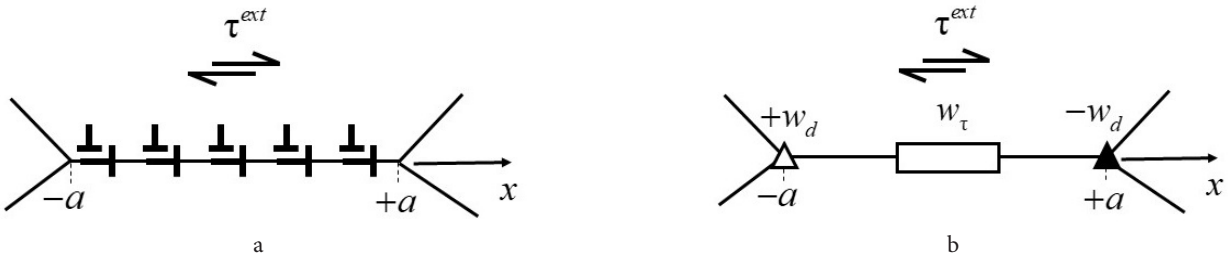

Fig. 1. Schematic plot of sessile and glissile components of dislocations accumulating at the boundary during intragranular plastic deformation (a) and their equivalent mesodefects (b) (the rectangle denotes a shear planar mesodefect, light and dark triangles are positive and negative disclination of the dipole, correspondingly), τ^{ext} is the external shear stress.

n_w and virtual unlike dislocations providing pure GBS. It is obvious that, the function $\rho_n(x_i)$ will converge to $\rho(x)$ with a decrease of b_d:

$$\rho(x) = \lim_{n\to\infty} \rho_n(x_i).$$

The numerical simulation procedure is as follows:

Stage 1. The equilibrium distribution of virtual dislocations is calculated using the method of successive approximations. The iteration procedure includes the following steps:

1.1. Determination of movable virtual dislocations of the mesodefect, (i.e. the acting force on these dislocations is greater than the threshold force: $|b_d\tau^\Sigma| > |b_d|\tau_0$). If there are no movable dislocations, equilibrium positions for all dislocations of the mesodefect are found.

1.2. Determination of the equilibrium state of a system of virtual dislocations by sorting in descending order of the force acting on them, and searching for the equilibrium position of each of these dislocations while the rest are fixed.

Stage 2. If the dislocations of the mesodefect in the equilibrium state are not distributed over the whole length of the boundary, pure GBS can occur on the remaining part of it.

Pure GBS was simulated by the following iteration procedure:

2.1. Sequential generation of pairs of unlike virtual dislocations with the same Burgers vector b_d as dislocations of the shear mesodefect according to the scheme shown in Fig. 2, and determination of the coordinates of dislocations at which the forces acting on them $b_d\tau^\Sigma$ are equal to the value $b_d\tau_0$ (Fig. 2). If no such coordinates are found, the iterative procedure is completed.

2.2. Search for the equilibrium of a system of dislocations, including both dislocations of a shear mesodefect and dislocations providing pure GBS according to the procedure described above.

The equilibrium distributions $\rho(x)$ were obtained for fixed parameters τ_0, w_τ, $2a$ at different increasing values of τ^{ext}. This procedure is repeated until the value of the external stress τ^{ext} reaches the value τ_{cr}, at which the sum of the Burgers vectors of virtual dislocations located in the interval $x_i \in [a-2r_0, a]$ becomes equal to $2b$. At $\tau^{ext} \geq \tau_{cr}$ a dislocation microcrack with the Burgers vector $B \geq 2b$ nucleates. The dislocation distribution calculated using the abovementioned iteration procedure may depend on the sequence of dislocation replacements specified by the equations of motion. In this regard, an additional study was carried out to estimate the effect of changing the sequence of selection of dislocations on the form of their final equilibrium distribution. The following metric was used to evaluate the proximity η of the distributions $\rho_d^{(1)}$ and $\rho_d^{(2)}$ obtained for two different arbitrarily chosen ways of dislocations motion:

$$\eta(\rho_n^{(1)}, \rho_n^{(2)}) = \frac{1}{n}\sum_{i=1}^{n}\left|x_i^{(1)} - x_i^{(2)}\right|,$$

where $x_i^{(1)}$, $x_i^{(2)}$ are the coordinates of discrete dislocations of distributions $\rho_n^{(1)}$ and $\rho_n^{(2)}$ correspondingly. The results of the analysis show that with a random choice of removable dislocations for a given discretization of the Burgers vector of dislocations, the value of $\eta(\rho_d^{(1)}, \rho_d^{(2)})$ changes insignificantly in comparison with the average distance between virtual discrete dislocations for different input parameters of the model. Thus, a change in the sequence of selection of movable dislocations has practically no effect on the form of their final equilibrium distribution $\rho(x)$.

4. Results and discussion

Numerical calculations were performed for a model material with the following values of the parameters: $G = 45000$ MPa, $\nu = 0.3$, $b = 3\cdot10^{-4}$ μm, $2a = 0.2 \div 1$ μm $w_\tau = 0.02 \div 0.04$. The discretization value of the Burgers vector was chosen equal to $b_d = 3\cdot10^{-5}$ μm. For comparison, the case of pure GBS in the absence of the shear mesodefect ($w_\tau = 0$) was also considered. The dependences of the critical external stress τ_{cr} on the mesodefect length $2a$, calculated for different mesodefect strengths w_τ at the threshold stress $\tau_0 = 0.8\cdot10^{-2}G$, are shown in Fig. 3. It can be seen that the presence of the mesodefect, providing strain-induced GBS, leads to a significant decrease in the critical stress τ_{cr} in comparison with the case of pure sliding.

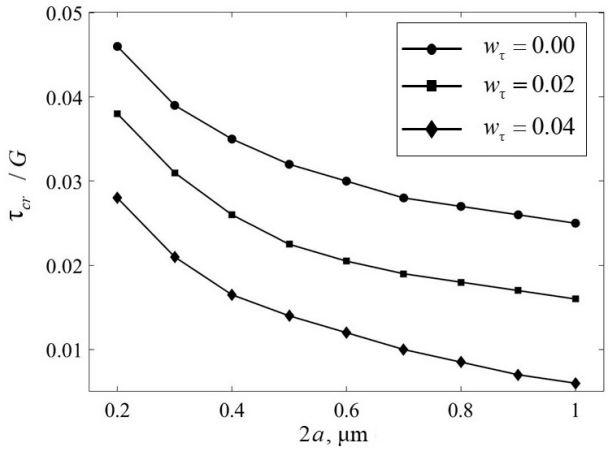

Fig. 3. Dependence of the critical stress of microcrack nucleation τ_{cr} on the mesodefect length $2a$ at different values of the mesodefect strength ($\tau_0 = 0.8\cdot10^{-2}G$).

Note that the distribution $\rho(x)$ depends on the parameters of the considered system (see Fig. 4 a, b, c, d). Thus, Fig. 4 a shows the distribution at $\tau^{ext} = \tau_{cr} = 3.1\cdot10^{-2}G$ for the parameters $2a = 0.3$ μm, $w_\tau = 0.02$ and $\tau_0 = 8\cdot10^{-3}G$. In this case both strain-induced and pure GBS take place. In contrast to the case in Fig. 4 a, the distribution shown in Fig. 4 b, calculated at a higher mesodefect strength, does not contain a negative part. This is explained by the fact that in this case, no pure GBS occurs. A small local increase in $\rho(x)$ is observed near the point $x = -0.15$ μm. Fig. 4 c shows $\rho(x)$ for the mesodefect parameters $2a = 0.8$ μm, $w_\tau = 0.04$ and the threshold stress $\tau_0 = 0.8\cdot10^{-2}G$. In general, its form resembles the distribution shown in Fig. 4 b, with the difference that there is a "shelf" on some part of the boundary (see Fig. 4 c). It is due to the total shear stress at any point of this part at each stage of the calculation was lower than the threshold stress and, therefore, the original uniform distribution of the Burgers vector density remains unchanged. Finally, Fig. 4 d shows the distribution in the case of pure GBS ($w_\tau = 0$). Note that this distribution differs from the well-known solution for

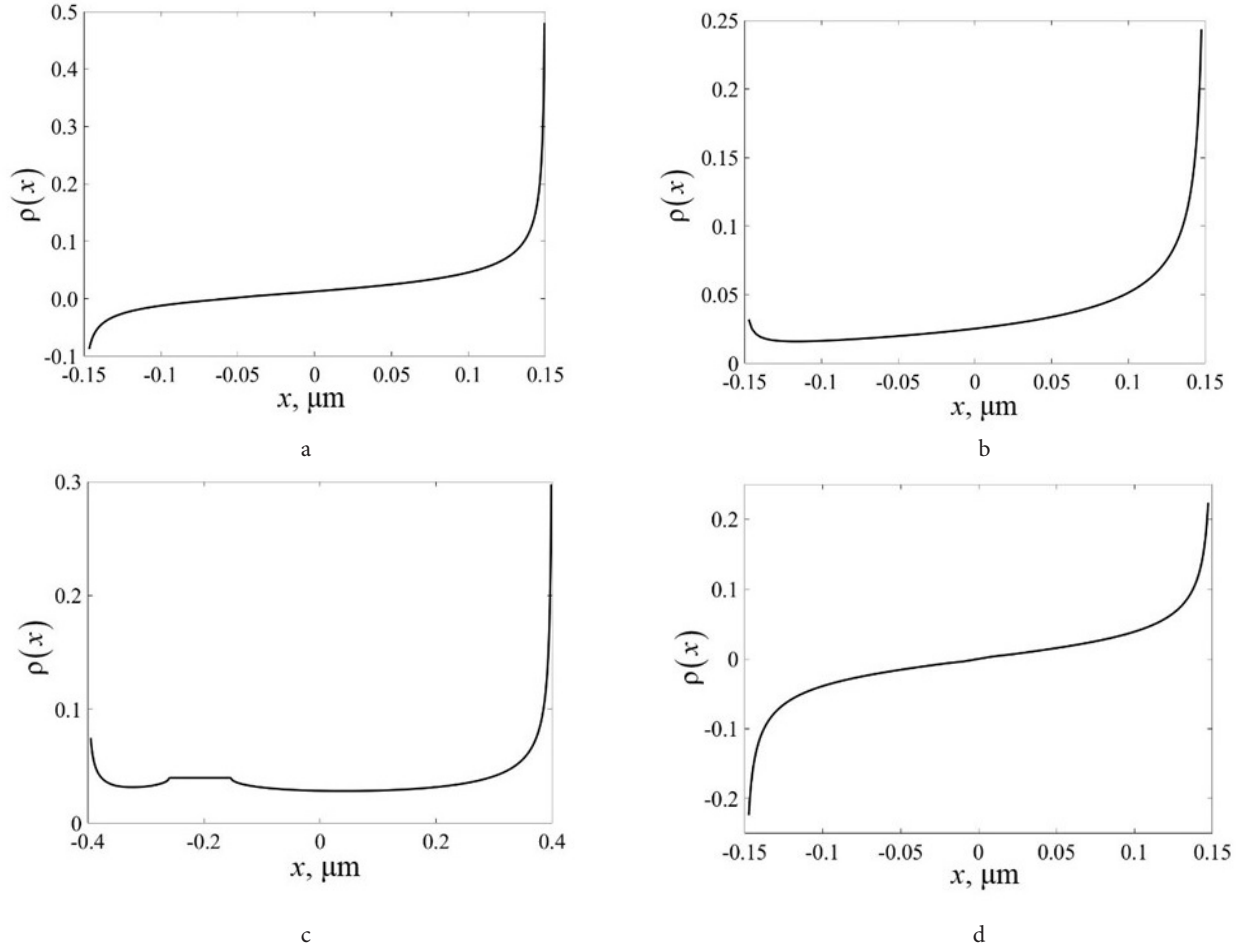

Fig. 4. The distribution $\rho(x)$ obtained for the following values of the system parameters: $\tau^{ext} = \tau_{cr} = 3.1 \cdot 10^{-2} G$, $2a = 0.3$ μm, $w_\tau = 0.02$ (a), $\tau^{ext} = \tau_{cr} = 2.1 \cdot 10^{-2} G$, $2a = 0.3$ μm, $w_\tau = 0.04$ (b), $\tau^{ext} = \tau_{cr} = 8.5 \cdot 10^{-3} G$, $2a = 0.8$ μm, $w_\tau = 0.04$ (c), $\tau^{ext} = \tau_{cr} = 3.9 \cdot 10^{-2} G$, $2a = 0.3$ μm, $w_\tau = 0$ (d) (the value τ_0 for all cases is the same and equal $\tau_0 = 0.8 \cdot 10^{-2} G$).

the bilateral dislocations pile-up [22] due to the presence of the threshold stress.

The dependence of the critical stress of crack nucleation τ_{cr} on the mesodefect length $2a$ at different values of the threshold stress and a fixed value $w_\tau = 0.04$ is shown in Fig. 5. It can be seen that an increase in the threshold stress of GBS τ_0 suppresses crack nucleation.

5. Conclusion

The investigation shows that the strain-induced athermal grain boundary sliding, carried out by the motion of glissile components of dislocations, accumulating at the grain boundaries during intragranular plastic deformation, can be considered as one of the possible mechanisms for the nucleation of microcracks in materials with a fragmented structure. These types of structures containing a large fraction of nonequilibrium strain-induced high angle grain boundaries are formed at large plastic deformations. The planar shear mesodefect play the main role in crack nucleation. Crack nucleation is possible when a certain critical value of the external stress is reached, which depends on the parameters of the system under consideration. A dipole of wedge disclinations does not create shear stresses at the boundary and, therefore, within the framework of the considered model, does not affect the motion of glissile dislocations. However, it must be taken into account when analyzing the characteristics of a crack arising at a grain junction. Consideration of more realistic grain boundary configurations and detailed analysis of microcrack characteristics will be carried out in future publications.

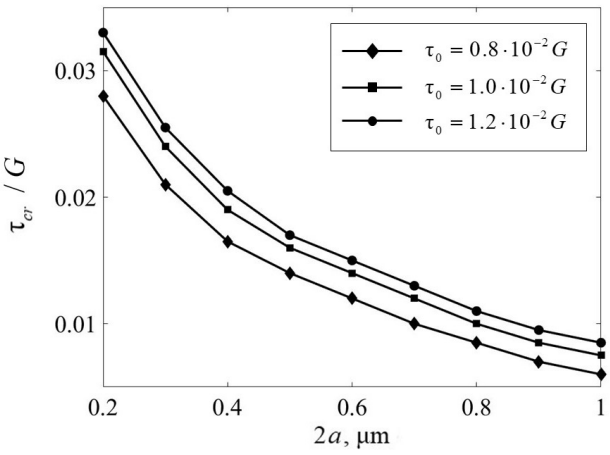

Fig. 5. Dependence of the critical stress τ_{cr} on the mesodefect length $2a$ at different values of the threshold stress and at $w_\tau = 0.04$.

Acknowledgements. This work was supported by the Russian Science Foundation, project No 21-19-00366.

References

1. V. V. Rybin. Large plastic deformations and fracture of metals. Moscow, Metallurgiya (1986) 223 p. (in Russian) [В. В. Рыбин. Большие пластические деформации и разрушение металлов. Москва, Металлургия (1986) 223 с.]
2. V. V. Rybin. Probl. Mater. Sci. 1 (33), 9 (2003).
3. V. V. Rybin, A. A. Zisman, N. Yu. Zolotorevsky. Acta Met. Mater. 41 (7), 2211 (1993). Crossref
4. A. A. Zisman, V. V. Rybin. Acta Mater. 44 (1), 403 (1996). Crossref
5. V. N. Perevezentsev, G. F. Sarafanov. Reviews on Advanced Materials Science. 30 (1), 73 (2012).
6. A. E. Romanov, A. I. Kolesnikova. Prog. Mater. Sci. 54, 740 (2009). Crossref
7. G. F. Sarafanov, V. N. Perevezentsev. Russian metallurgy (Metally). 10, 889 (2016). Crossref
8. M. Yu. Gutkin, I. A. Ovidko. Phil. Mag. Letters. 84 (10), 655 (2004). Crossref
9. A. A. Nazarov, M. S. Wu, K. Zhou. Phys. Met. Metallogr. 104 (3), 274 (2007). Crossref
10. M. S. Wu. International Journal of Plasticity. 100, 142 (2018). Crossref
11. S. V. Kirikov, V. N. Perevezentsev. Lett. Mater. 11 (1), 50 (2021). (in Russian) [С. В. Кириков, В. Н. Перевезенцев. Письма о материалах. 11 (1), 50 (2021).] Crossref
12. I. A. Ovid'ko, A. G. Sheinerman. Physics of the Solid State. 49 (6), 1111 (2007). Crossref
13. I. A. Ovid'ko, A. G. Sheinerman. Acta Materialia. 52, 1201 (2004). Crossref
14. M. B. Ivanov, Yu. R. Kolobov, S. S. Manokhin, E. V. Golosov. Inorganic Materials. 49 (15), 1320 (2013). Crossref
15. T. Matsunaga, T. Kameyama, S. Ueda, E. Sato. Philos. Mag. 90, 4041 (2010). Crossref
16. J. Koike, R. Ohyama, T. Kobayashi, M. Suzuki, K. Maruyama. Mater. Trans. 44, 445 (2003). Crossref
17. J. Koike. Metall. Mater. Trans. A. 36, 1689 (2005). Crossref
18. N. Stanford, K. Sotoudeh. P. S. Bate. Acta Mater. 59, 4866 (2011). Crossref
19. V. Doquet, B. Barkia. Mech. Mater. 103, 18 (2016). Crossref
20. S. Hémery, C. Tromas, P. Villechaise. Materialia. 5, 100189 (2019). Crossref
21. C. Zener. In: Fracturing of Metals (Ed. by F. Jonassen, W.P. Roop, R.T. Bayless). The American Society for Metals, Cleveland, OH (1948), pp. 3–31.
22. J. P. Hirth, J. Lothe. Theory of dislocations. New York, Wiley (1982) 839 p.